Journal of ELECTRONIC MATERIALS, Vol. 45, No. 12, 2016
DOI: 10.1007/s11664-016-4815-8

Influence of Li Addition to Zn-Al Alloys on Cu Substrate During Spreading Test and After Aging Treatment

TOMASZ GANCARZ,[1,4,5] JANUSZ PSTRUS,[1] GRZEGORZ CEMPURA,[2] and KATARZYNA BERENT[3]

1.—Institute of Metallurgy and Materials Science, Polish Academy of Sciences, 30-059 Kraków, Poland. 2.—International Centre of Electron Microscopy for Materials Science, Faculty of Metals Engineering and Industrial Computer Science, AGH University of Science and Technology, Kraków, Poland. 3.—Academic Centre for Materials and Nanotechnology, AGH University of Science and Technology, 30-059 Kraków, Poland. 4.—e-mail: nmgancar@imim-pan.krakow.pl. 5.—e-mail: t.gancarz@imim.pl

The spreading of Zn-Al eutectic-based alloys with 0.05 wt.%, 0.1 wt.%, and 0.2 wt.% Li on Cu substrate has been studied using the sessile drop method in presence of QJ201 flux. Wetting tests were performed after 1 min, 3 min, 8 min, 15 min, 30 min, and 60 min of contact at temperatures of 475°C, 500°C, 525°C, and 550°C. Samples after spreading at 500°C for 1 min were subjected to aging for 1 day, 10 days, and 30 days at temperature of 120°C, 170°C, and 250°C. The spreadability of eutectic Zn-5.3Al alloy with different Li contents on Cu substrate was determined in accordance with ISO 9455-10:2013-03. Selected solidified solder–substrate couples were, after spreading and aging tests, cross-sectioned and subjected to scanning electron microscopy, energy-dispersive spectroscopy (EDS), and x-ray diffraction (XRD) analysis of the interfacial microstructure. An experiment was designed to demonstrate the effect of Li addition on the kinetics of the formation and growth of CuZn, Cu_5Zn_8, and $CuZn_4$ intermetallic compound (IMC) phases, during spreading and aging. The IMC layers formed at the interface were identified using XRD and EDS analyses. Increasing addition of Li to Zn-Al alloy caused a reduction in the thickness of the IMC layer at the interface during spreading, and an increase during aging. The activation energy was calculated, being found to increase for the Cu_5Zn_8 phase but decrease for the CuZn and $CuZn_4$ phases with increasing Li content in the Zn-Al-Li alloys. The highest value of 142 kJ mol^{-1} was obtained for Zn-Al with 1.0 Li during spreading and 69.2 kJ mol^{-1} for Zn-Al with 0.05 Li during aging. Aging at 250°C caused an increase in only the Cu_5Zn_8 layer, which has the lowest Gibbs energy in the Cu–Zn system. This result is connected to the high diffusion of Cu from the substrate to the solder.

Key words: Zn-Al-Li, spreading test, lead-free solder, IMCs, aging, microstructure

INTRODUCTION

Addition of Li to Al alloys,[1–3] Mg alloys,[4–6] and Zn-Al alloys[7] can improve their mechanical properties,[1–6] increase their thermal properties[1–6] during aging[1,2] and soldering,[8] and reduce their density.[1] For Al alloys, the high concentration and significant vacancy-binding energy of Li atoms cause preferential clustering between Li atoms and quenched-in vacancies, thus retarding diffusion of Zn and Mg atoms and thereby suppressing homogeneous nucleation of Zn-rich phases in the matrix.[1] Al-Li-Zn-Mg-Cu alloys show comparable tensile properties to but

(Received April 19, 2016; accepted July 18, 2016; published online August 4, 2016)

7% lower density than 7075 alloy.[1] In the case of Mg alloys, AZ31 alloy with 5% Li content possessed the smallest planar anisotropy and enhanced ductility.[4] The excellent tensile properties of AZ31 alloys with Li addition were mainly attributed to the regularly arranged, grained, recrystallized microstructure.[4] Intermetallic compounds (IMCs) of Li, such as Al_3Li[1–3,9] or $MgLi_2X$,[4–6] have the main impact in terms of increasing the mechanical properties. They also have significant influence on aging and the plastic deformation process. However, the IMCs also increase the electrical resistivity, linear coefficient of thermal expansion (CTE), and hardness,[7] and most importantly could block the increase of intermetallic layers, essential to the soldering process, at the solder–substrate interface.[10] The characteristics of cast Zn-Al alloys with Li additions were presented in Ref. 7, revealing Al_3Li, AlLi precipitates, and lamellar eutectic Zn-Al structure ($\alpha + \eta$) in the microstructure. Mechanical and thermal properties increased with increasing Li content. In literature data, there is no information about the influence of Li addition on the formation and growth of IMC layers during the soldering process. During a similar spreading process, added Ag,[10] Cu,[11] and Na[12] formed an IMC with Zn that blocked the growth of an IMC from the Cu-Zn system layer at the interface. The resulting $AgZn_3$, Cu_5Zn_8 and $CuZn_4$, and $NaZn_{13}$ precipitates, in Zn-Al-Ag,[10] Zn-Al-Cu,[11] and Zn-Al-Na,[12] respectively, blocked diffusion of Zn to the interface, which was connected with the Zn in the IMCs. On transmission electron microscopy investigation of the microstructure of Zn-Al-Li cast alloys, very small precipitates were found in the Zn area; although they could not be identified, they might be IMCs from the Li–Zn system,[13] such as Li_2Zn_3, $LiZn_2$, Li_2Zn_5, and $LiZn_4$, or the ternary Al–Li–Zn system,[13] such as τ_1 ($Li_{1+x}Zn_{0.5-1.5}Al_{0.5-1.5}$), τ_2 ($LiZn_{0.6-0.8}Al_{0.4-0.2}$), τ_3($LiZn_3Al$), and τ_4 (Li_3ZnAl_5). Calorimetry measurements[7] revealed a widening of the characteristic peaks, at around 280°C for the α to α' reaction and around 380°C for the melting reaction,[14] which could correspond to liq. + Al_2Li_3 $\rightarrow$ Al_4Li_9 + AlLi and liq. $\rightarrow$ τ_3 + hcp + β-$LiZn_4$, respectively.[7]

Zn-base solders with alloying elements were further developed for ultrahigh-temperature applications.[15] Previous studies on Zn-Al-Ag,[10] Zn-Al-Cu,[11] and Zn-Al-Na[12] and literature data for Zn-Al-Cu[16,17] and Zn-Al-Mg-Ga[18] describe the influence of time, temperature, and alloying elements in the spreading process on the spreadability and the growth of the IMC layers at the interface. These studies reveal that small addition of alloying elements reduces the IMC layers at the interface, and that increasing time and temperature caused increasing diffusion of Cu to the solder and the growth of IMC layers, most notably the Cu_5Zn_8 layer, which has the lowest Gibbs energy.[11] Moreover, the Al–Li precipitates formed in the solder could block diffusion of Al to the interface, which should slow down formation of Al_4Cu_9 phase at the interface inside the Cu_5Zn_8 layer. This is in accordance with the phase diagram of the Al–Cu–Zn system.[19] The aim of this study is to demonstrate the effect of Li addition on the kinetics of formation and growth of the CuZn, Cu_5Zn_8, and $CuZn_4$ phases, in the spreading process and after aging treatment.

EXPERIMENTAL PROCEDURES

Cast eutectic Zn-5.3Al alloys with 0.05 wt.%, 0.1 wt.%, and 0.2 wt.% Li[7] (Zn-Al + Li) were studied in air using the sessile drop method in presence of QJ201 flux. Experiments without flux were unsuccessful, as the solder surface oxidized, resulting in failure to connect with the Cu substrate. Therefore, QJ201 flux from powder, consisting of 50 wt.% KCl, 32 wt.% LiCl, 10 wt.% NaF, and 8 wt.% $ZnCl_2$, was applied for protection and oxide removal. Spreading tests were performed after 1 min, 3 min, 8 min, 15 min, 30 min, and 60 min of contact at temperatures of 475°C, 500°C, 525°C, and 550°C. As described in Refs. 7 and 10, the spreading area of 0.5-g samples of Zn-Al-Li solder was calculated after cleaning flux residue from solidified samples. The spreading area was calculated using the Get Area script in CorelDRAW 12. The margin of error for measurements was 5%, as described in Ref. 10. The time and temperature dependence of the spreadability of Zn-Al + Li on Cu was determined. Samples after the spreading test at 500°C for 1 min were subjected to aging for 1 day, 10 days, and 30 days at 120°C, 170°C, and 250°C. The aging process was conducted in an electrical furnace in air. Half of the selected samples were placed in the furnace for the appropriate time and at the appropriate temperature. The growth rate and activation energy of the Cu_5Zn_8 layer in solid state were determined during the spreading test and aging. Selected solder–substrate couples were cut perpendicular to the plane of the interface using a diamond wire saw, then mounted in conductive resin, ground, polished, covered with a thin layer of C to protect from oxygen, and subjected to microstructural and elemental analyses by scanning electron microscopy (SEM) coupled with energy-dispersive spectrometry (EDS) and x-ray diffraction (XRD) analysis, to study the interfacial microstructure and IMCs occurring at the interface. The thickness of the IMC layer (D) is dependent on the growth rate (k) and growth time (t) with an exponential factor (n):

$$D = k(t)^n. \tag{1}$$

The growth rate for interface migration can be described by an Arrhenius-type equation (2):

$$k = k_0 \exp\left(-\frac{Q}{RT}\right), \tag{2}$$

where k_0, Q, R, and T represent the migration rate constant, the activation energy, the universal gas constant, and absolute temperature, respectively.

The initial thickness of each IMC layer after the aging process should be taken into account, and Eq. 1 should be modified to

$$\Delta x = d_0 + kt^n, \quad (3)$$

where Δx is the average thickness of the IMC layer, d_0 is the initial thickness of the IMC layer, k is the growth rate coefficient, and t is the aging duration.

RESULTS AND DISCUSSION

Spreading Test

In previous study,[7] the characteristics of cast Zn-Al-Li alloys were presented. The influence of Li addition on the thermal and mechanical properties, which were increased due to the formation of IMC precipitates, can be seen in the microstructure using transmission electron microscopy and XRD. However, the high reactivity of Li, the impossibility of using EDS analysis, and the lack of literature and crystal structure data mean that only AlLi and Al_3Li precipitates could be identified in cast Zn-Al-Li alloys.[7] Furthermore, calorimetry measurements showed the possibility that the τ_3 present corresponds to $LiZn_3Al$, which could have a decisive impact on the diffusion of Zn to the interface.[7] The connection of Zn with the formed IMCs, as shown in Ref. 10 for Ag addition, causes a reduction in the thickness of IMC layers at the interface. Regarding the soldering process, the spreading area of Zn-Al-Li alloys for the spreading test at 500°C after 1 min, 3 min, 8 min, 15 min, 30 min, and 60 min of contact, and at temperatures of 475°C, 500°C, 525°C, and 550°C after 8 min, are shown in Fig. 1a and b, respectively. Generally, compared with eutectic Zn-Al, increased spreading area was observed for Zn-Al alloys with Li addition. The highest growth in the time and temperature dependences was observed for Zn-Al-0.05 wt.%Li. However, increasing the Li content in the eutectic Zn-Al caused the spreading area to reduce, reaching its lowest value for Zn-Al-0.2Li. Similar effects have been observed in terms of reduced spreading area with increasing addition of Ag[10] and Cu[16] to eutectic Zn-Al. This could result in creation of IMC precipitates which are not dissolved in the solder during the spreading test, or short-range ordering (creation of associates) in the liquid.[20] These two mechanisms reduce the volume of liquid and increase its density,[20] which reduces the spreading area.

Figure 2 shows the cross-sectional microstructure of Zn-Al with 0.05 wt.% Li alloy on Cu substrates after the spreading test at temperature of 500°C for times of (a) 1 min, (b) 3 min, (c) 8 min, (d) 15 min, (e) 30 min, and (f) 60 min. In the microstructure at the solder–Cu substrate interface, IMC layers from the Cu–Zn system form. Three IMC layers (CuZn, Cu_5Zn_8, and $CuZn_4$) were observed to occur at the interface from the Cu substrate side, as shown in previous work and literature data.[10–12,15,17,21] All IMC layers grew with increasing time, with the highest growth for the Cu_5Zn_8 layer; similar thickness of Cu_5Zn_8 layer was observed in literature data.[10–12,15,17,21] Analysis of Li by SEM–EDS was below the detection level, so EDS analysis of Li is not reported in Table I. At the beginning of spreading (1 min to 8 min), the thicknesses of Cu_5Zn_8 and $CuZn_4$ were similar. With increasing time (15 min to 60 min), Cu_5Zn_8 grew the fastest, due to the diffusion of Cu and its having the lowest Gibbs energy of the phases formed at the interface.[10,12] Similar to earlier work on Zn-Al with Ag,[10] Cu,[11,17] Na[12] and Si,[22] three IMCs from the Cu–Zn system formed at the interface. The $CuZn_4$ layer with scallop-shaped morphology, which become detached and moved into the solder, and the greater thickness of the Cu_5Zn_8 phase, show the fast path for Cu diffusion and the thin, smooth CuZn layer.

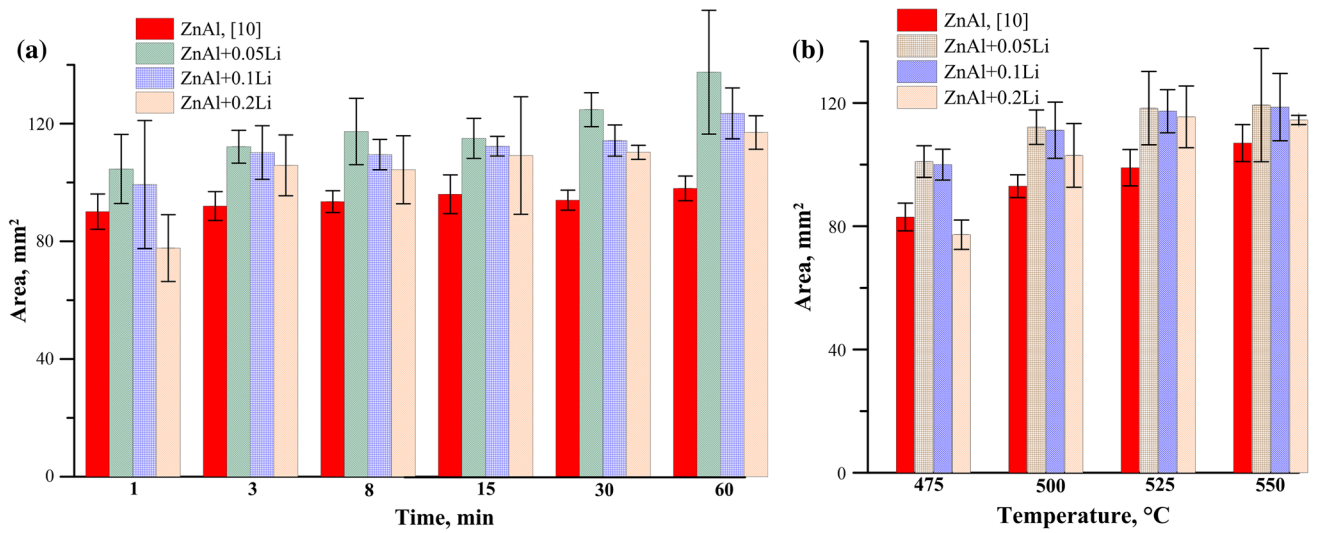

Fig. 1. Spreading area of Zn-Al alloys with Li addition: (a) time and (b) temperature dependence.

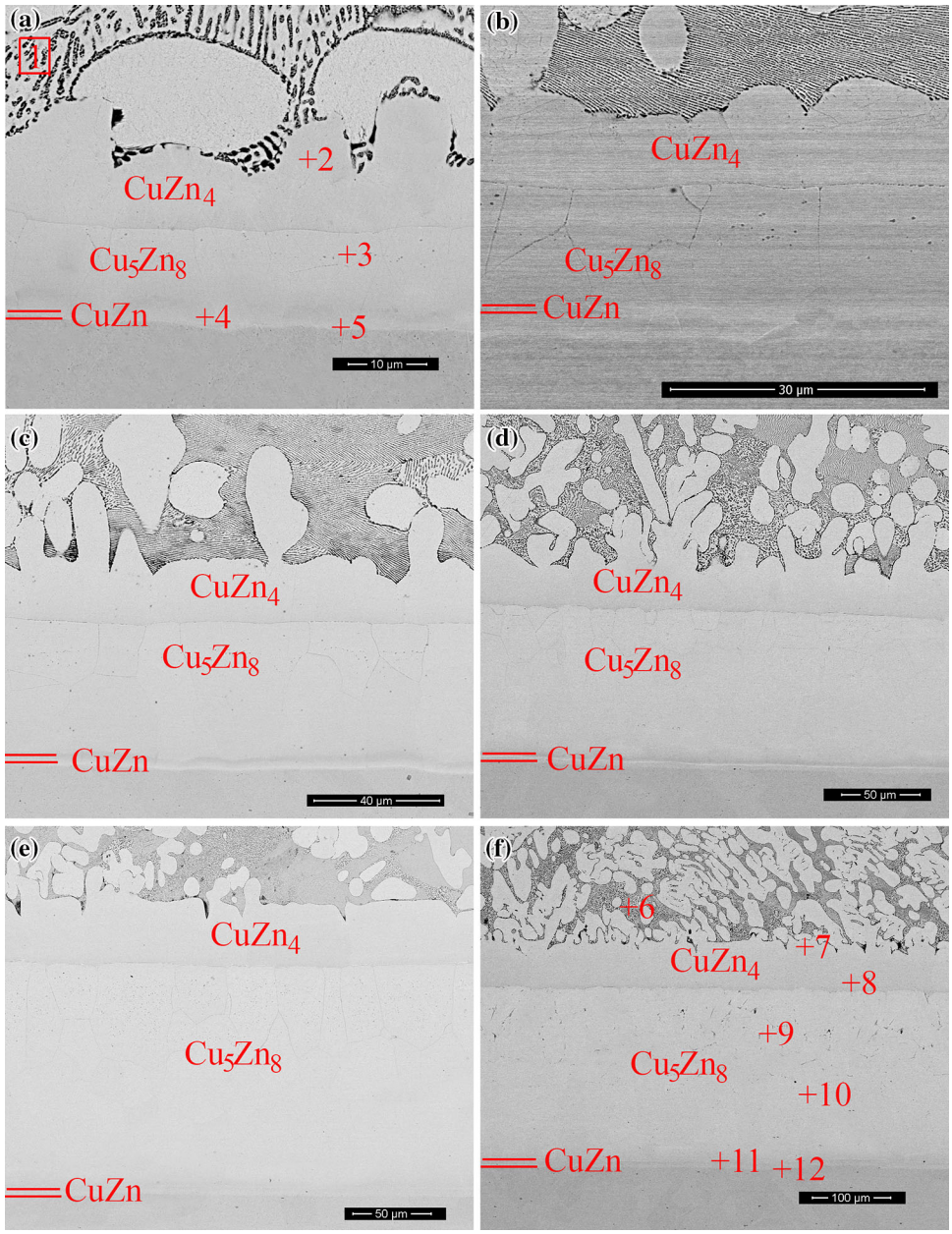

Fig. 2. Microstructure of interfaces on cross-sections of Zn-Al + 0.05Li alloy on Cu substrate after spreading test at temperature of 500°C for times of (a) 1 min, (b) 3 min, (c) 8 min, (d) 15 min, (e) 30 min, and (f) 60 min, with IMCs and EDS analysis points marked (values presented in Table I).

However, the different character of the IMC layer formed at the beginning of spreading has a significant impact on the growth and the diffusion of Cu to the interface.

Figure 3a–c presents the thicknesses of the IMC layers formed at the interface at temperature of 500°C and time from 1 min to 60 min, for Zn-Al with 0.2 wt.%, 0.5 wt.%, and 1.0 wt.% Li addition, respectively. At the beginning of the spreading test (1 min to 8 min), the thicknesses of the Cu_5Zn_8 and $CuZn_4$ layers are almost the same. After 15 min, the Cu_5Zn_8 was the thickest. A different character of the growth of IMC layers was observed for Zn-Al + Ag[10] and Zn-Al + Na,[12] with higher growth of Cu_5Zn_8 being observed after just 3 min. This could be caused by Cu–Zn system layers formed above the interface. Figure 4 shows the high amount of Al–Li precipitates, which block diffusion of Zn to the interface and inhibit the growth of the $CuZn_4$ and Cu_5Zn_8 phases. Preparation of foils for TEM microstructure observations was very difficult because the samples were brittle and cracked at the interface as a result of residual stresses, as indicated by the scanning transmission electron microscopy (STEM) images in Fig. 4a. According to Date et al.,[23] the observed Cu_5Zn_8 layer thickening

Table I. EDS analysis of Zn-Al alloys with Li at points marked in Figs. 2, 5, and 8–10

Marked point	wt.%			at.%		
	Al^K	Cu^K	Zn^K	Al^K	Cu^K	Zn^K
1	8.1	4.1	87.9	17.5	3.7	78.8
2	1.2	17.4	81.5	2.7	17.5	79.8
3	4.0	41.3	54.8	9.0	39.7	51.3
4	8.3	55.6	36.1	17.8	50.4	31.8
5	4.4	47.5	48.1	9.9	45.4	44.7
6	10.6	3.7	85.7	22.3	3.3	74.4
7	1.7	19.4	79.0	3.9	19.4	76.7
8	3.1	29.2	67.6	7.2	28.6	64.3
9	13.1	54.4	32.5	26.4	46.6	27.0
10	4.5	47.1	48.4	10.2	45.0	44.9
11	3.0	55.4	41.6	6.8	53.9	39.3
12	2.0	57.9	40.0	4.7	57.0	38.3
13	8.1	3.7	88.2	17.6	3.4	79.0
14	1.2	18.2	80.7	2.8	18.3	78.9
15	1.7	21.5	76.9	4.0	21.4	74.6
16	5.9	49.3	44.9	12.9	46.2	40.9
17	8.0	55.6	36.4	17.1	50.7	32.2
18	4.4	52.0	43.6	9.9	49.6	40.5
19	6.3	3.6	90.1	14.0	3.4	82.6
20	2.7	26.3	70.9	6.3	25.9	67.8
21	1.2	34.1	64.8	2.8	34.1	63.1
22	5.3	48.8	45.9	11.8	46.0	42.2
23	7.6	58.0	34.5	16.3	53.0	30.7
24	5.3	55.1	39.6	11.8	51.9	36.3
25	7.1	3.0	89.9	15.7	2.8	81.6
26	1.0	15.7	83.3	2.5	15.8	81.7
27	1.3	17.9	80.8	3.1	18.0	78.9
28	2.1	22.5	75.5	4.8	22.3	72.9
29	3.3	40.9	55.8	7.6	39.7	52.7
30	3.8	41.9	54.3	8.7	40.4	50.9
31	8.6	56.0	35.4	18.3	50.6	31.1
32	5.7	49.8	44.6	12.6	46.8	40.7
33	9.4	3.7	87.0	20.0	3.3	76.7
34	2.1	2.5	95.4	5.0	2.5	92.5
35	1.6	18.5	79.8	3.9	18.5	77.6
36	0.9	33.3	65.8	2.0	33.6	64.4
37	23.7	63.4	12.9	42.4	48.1	9.5
38	12.7	62.4	25.0	25.6	53.5	20.9
39	6.0	47.7	46.4	13.2	44.6	42.2
40	8.6	4.8	86.6	18.5	4.4	77.1
41	1.5	3.8	94.7	3.5	3.9	92.7
42	1.3	18.6	80.1	3.2	18.6	78.2
43	0.7	19.8	79.5	1.6	20.1	78.3
44	1.4	36.9	61.7	3.3	36.8	59.9
45	11.5	55.6	33.0	23.6	48.5	28.0
46	5.7	48.8	45.5	12.7	45.8	41.5
47	26.9	48.3	24.8	46.6	35.6	17.8
48	1.8	4.3	93.9	4.3	4.3	91.5
49	8.2	5.3	86.6	17.7	4.9	77.5
50	34.7	56.1	9.3	55.7	38.2	6.1
51	13.8	72.8	13.4	27.5	61.5	11.0
52	1.1	38.7	60.2	2.7	38.7	58.6
53	1.3	39.1	59.6	3.0	39.1	58.0
54	10.4	3.9	85.7	21.9	3.5	74.6
55	0.6	3.0	96.4	1.4	3.1	95.5
56	67.5	0.0	32.5	83.4	0.0	16.6
57	32.5	56.8	10.7	53.2	39.5	7.3
58	11.9	55.2	32.9	24.3	47.9	27.8
59	2.1	39.7	58.2	4.8	39.3	55.9
60	2.2	39.7	58.1	5.1	39.2	55.8

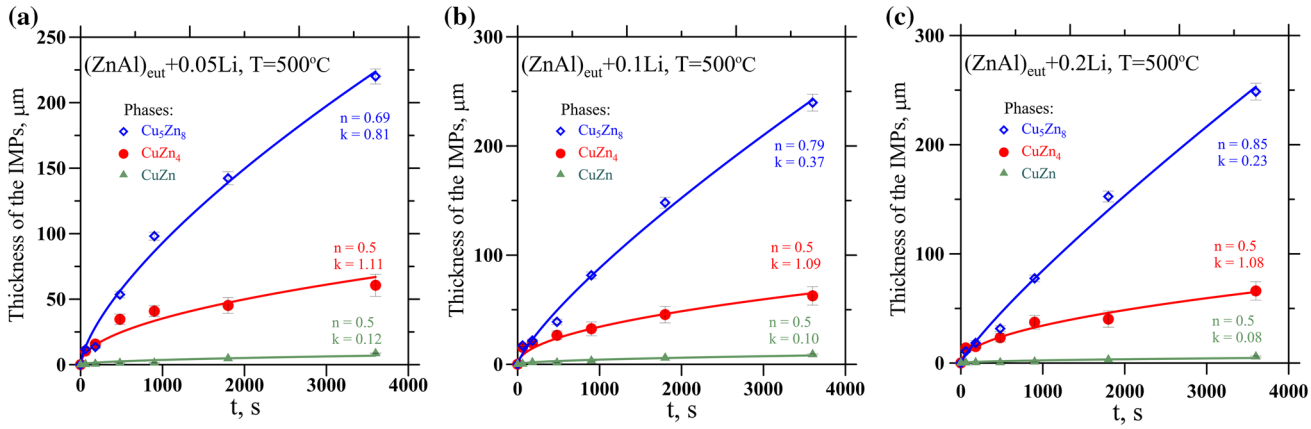

Fig. 3. Dependence of IMC thicknesses on time for (a) 0.05 wt.%, (b) 0.1 wt.%, and (c) 0.2 wt.% Li addition to eutectic Zn-Al.

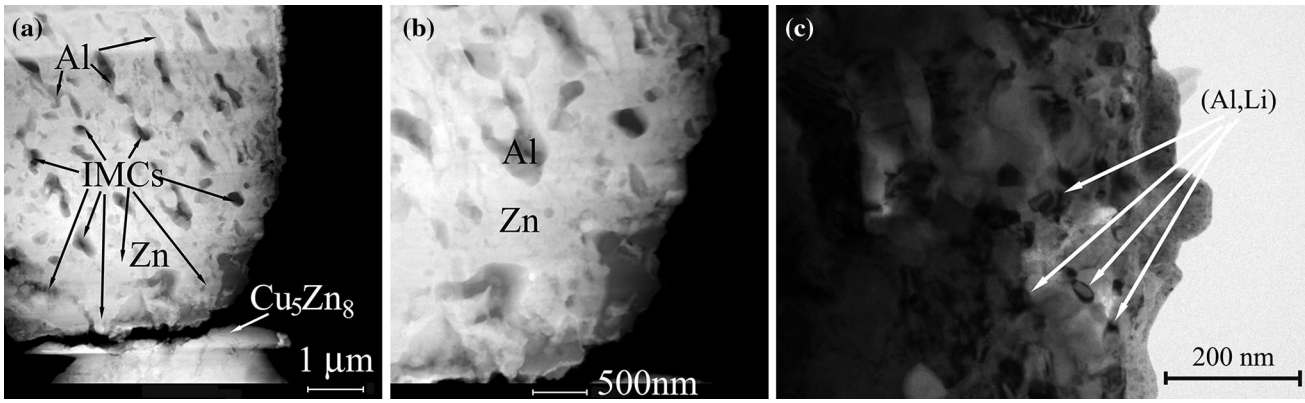

Fig. 4. TEM microstructure: (a, b) scanning transmission electron microscopy (STEM), (c) high-angle annular dark field (HAADF).

and void formation accounted for the brittleness of the solder/Cu. The precipitates from the Al–Li system observed in the high-angle annular dark field (HAADF) image in Fig. 4c were identified in cast alloys as Al_3Li and AlLi.[7] Moreover, the lowest thickness of IMC layers (289.3 μm) was obtained for 0.05 wt.% Li content. With increasing Li content in the Zn-Al-Li alloys, the thickness increased slightly (to 311.5 μm and 320.6 μm for 0.1 wt.% and 0.2 wt.% Li, respectively) after 60 min. The obtained thicknesses of the IMC layers were slightly lower compared with eutectic Zn-Al,[10] but similar to Zn-Al with addition of Ag,[10] Cu,[17] and Na.[12] The greatest growth of Cu_5Zn_8 corresponds to the highest stability of the Cu_5Zn_8 phase and high diffusion of Cu and Zn to the interface. The n parameter indicates the diffusion character, with $n = 0.5$ indicating control by volume diffusion and $n = 1$ a chemical reaction. For the Cu_5Zn_8 phase, increase in the n parameter with increasing Li addition was observed, being 0.69, 0.79, and 0.85 for 0.05 wt.%, 0.1 wt.%, and 0.2 wt.% Li. This rise of n corresponds to increasing chemical reaction in the formation process of the Cu_5Zn_8 layer with increasing Li addition. This could be caused by precipitates of Al-Li, corresponding to the higher amount of Zn in the Zn-Al + Li alloys. For Zn-Al + Ag,[10] Zn-Al + Cu,[11,17] and Zn-Al + Na,[12] addition of Ag, Cu, and Na resulted in creation of Ag–Zn, Cu–Zn, and $NaZn_{13}$ IMC, respectively, reducing the diffusion of Zn by bonding it with Ag, Cu or Na. The n value for $CuZn_4$ and CuZn was 0.5, meaning that the reaction was controlled by volume diffusion. The growth rate k reduced with increasing Li content in the Zn-Al + Li alloys for all IMCs (CuZn, Cu_5Zn_8, and $CuZn_4$ phases). The same situation was observed for the $CuZn_4$ phase for Zn-Al + Na,[12] but for the Cu_5Zn_8 phase, k remained at the same level (0.5) with increasing Na content. In the case of the Cu_5Zn_8 phase, addition of Na to Zn-Al alloys had no influence on the growth rate, meaning that, for shorter time, the Cu_5Zn_8 phase grows at the same rate and the only change is the diffusion character. A different character was observed for Zn-Al + Li alloys for the Cu_5Zn_8 phase. With increasing Li content, the growth rate reduced, causing lower thickness for short spreading times (up to 15 min), as shown in Fig. 3.

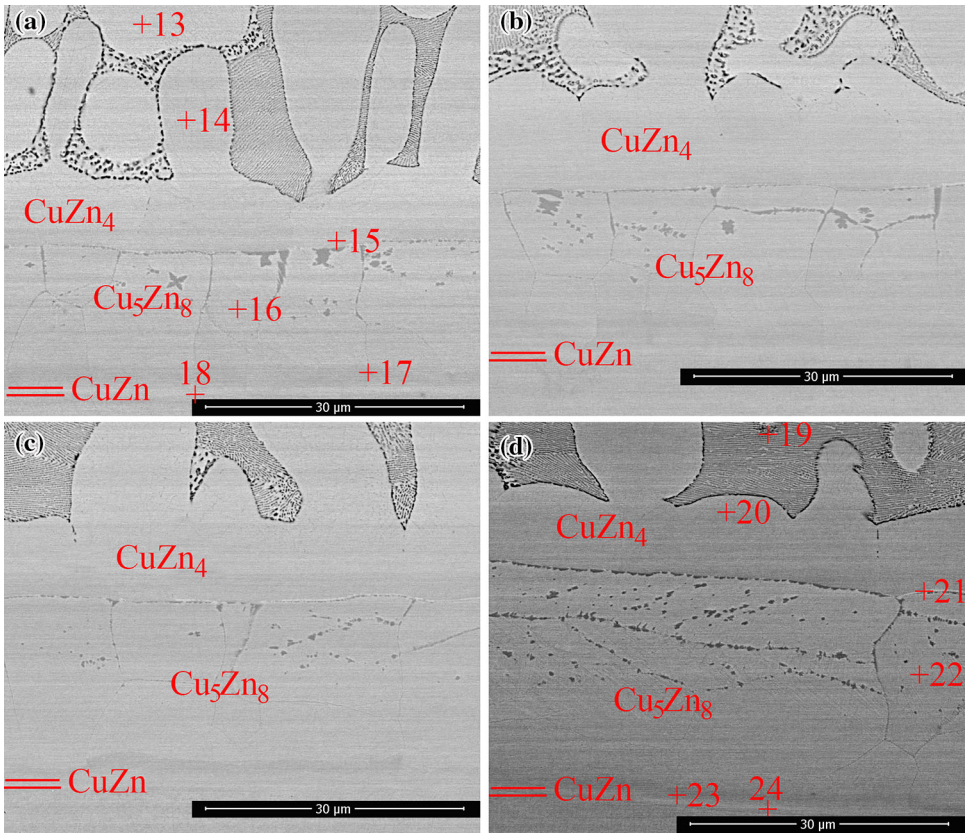

Fig. 5. Microstructure of interfaces on cross-sections of Zn-Al alloy with 0.2% Li on Cu substrate after spreading test for 8 min at temperature of (a) 475°C, (b) 500°C, (c) 525°C, and (d) 550°C, with IMCs and EDS analysis points marked (values presented in Table I).

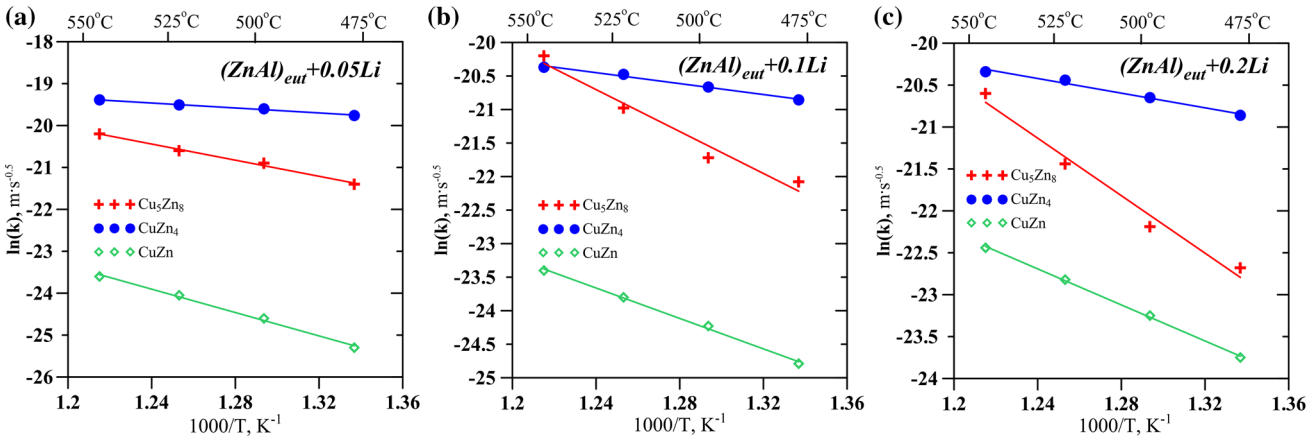

Fig. 6. Growth kinetics of IMC versus temperature for Zn-Al + Li alloys with (a) 0.05 wt.%, (b) 0.1 wt.%, and (c) 0.2 wt.% Li addition.

The microstructure of Zn-Al with 0.2% Li on a Cu substrate after spreading for 8 min at temperature of (a) 475°C, (b) 500°C, (c) 525°C, and (d) 550°C is presented in Fig. 5. The microstructure after the spreading test was similar for all Li contents, and IMC layers increased with increasing temperature. Similar to Refs. 10–12, 17, and 22, three IMCs (CuZn, Cu_5Zn_8, and $CuZn_4$ phases) formed from the Cu substrate at the interface. For all temperatures, the observed IMC layers looked the same: a smooth thin CuZn layer, a thick Cu_5Zn_8 layer with Al content caused by the fast path for Cu diffusion, and a $CuZn_4$ layer with scallops in the top. EDS analysis revealed the presence of more than 10 at.% Al, not only in the Cu_5Zn_8 but also in the CuZn phase, in accordance with the Al–Cu–Zn phase diagram,[19] which shows that Al dissolves in the Cu_5Zn_8 and CuZn phases. Close to the interface from the solder side, EDS analysis at points 13 (Fig. 5a) and 19 (Fig. 5d) showed higher amounts of Al and also

dissolved Cu. For all temperatures, in the Cu_5Zn_8 layer, there is a fast path for Cu diffusion, with EDS analysis revealing higher amounts of Al compared with the rest of the Cu_5Zn_8 layer. To identify the growth kinetics of the IMC layer and the activation energy, the dependence of ln k on inverse temperature is presented in Fig. 6a–c for the Zn-Al + Li alloys. The activation energies calculated for β-CuZn, γ-Cu_5Zn_8, and ε-$CuZn_4$ are presented in Table II. The activation energies for the β- and γ-phases for the Zn-Al + Li alloys are much higher than for eutectic Zn-Al,[10] and are only similar for the ε-phase. With increasing Li addition to the Zn-Al alloy, the activation energy is reduced for β-phase, but at the same time increases for γ- and ε-phases, inhibiting nucleation and growth of these phases at the interface. This confirms that Li addition has an effect on the formation of IMCs. A similar effect was observed for Zn-Al with Ag[10] and Na,[12] indicating that the IMC precipitates formed with Zn in the solder had a significant effect on the growth kinetics of IMC layers at the interface.

Table II. Activation energy of IMCs of Zn-Al alloys with different Li contents after spreading test

Alloy	IMC	Activation energy (kJ mol^{-1})
Zn-Al-0.05Li	β	115.9
	γ	79.9
	ε	24.6
Zn-Al-0.1Li	β	94.3
	γ	129.9
	ε	33.9
Zn-Al-0.2Li	β	89.3
	γ	142.6
	ε	36.4

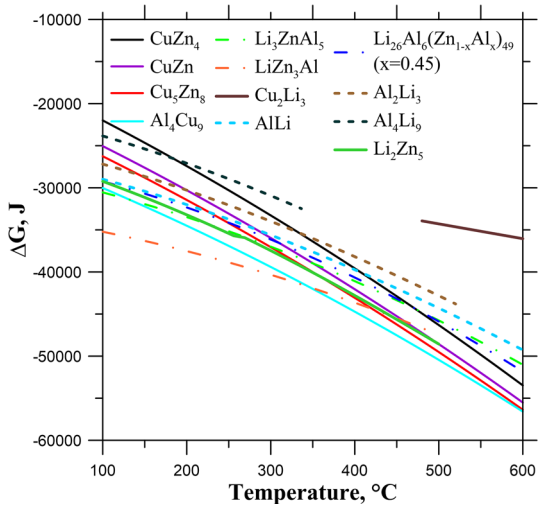

Fig. 7. Temperature dependence of Gibbs energy of IMCs, calculated with ThermoCalc using thermodynamic data from Refs. 13 and 19.

Considering the spreading process on a Cu substrate, one is dealing with two systems. One is Al–Zn–Li, which corresponds to the phases formed in the solder, and the second is Al–Cu–Zn, for the IMC layer formed at the interface. Taking into account the Gibbs energies of formation of the intermetallics, as discussed in Ref. 10, calculations using ThermoCalc and the thermodynamic parameters from Ref. 13 for the Al–Li–Zn system and from Ref. 19 for the Al–Cu–Zn system are presented in Fig. 7. These calculations indicate that $LiZn_3Al$ has the lowest Gibbs energy, which means it is thermodynamically the most stable in the solder, and the Al_4Cu_9 correlates to the Cu_5Zn_8 at the interface. Precipitates of the Al–Li, Li–Zn, and Al–Li–Zn systems were confirmed by their observation in the microstructure of Zn-Al-Li cast alloys,[7] but without literature and crystal structure data, it is impossible to identify the IMC precipitates occurring for cast Zn-Al-Li alloys. Selected-area electron diffraction (SAED) analysis made it possible to identify and confirm the occurrence of AlLi and Al_3Li precipitate phases. However, the very small precipitates inside the Zn area were not identified. The soldering process can be divided into two stages: first, dissolution of the Cu substrate by liquid solder, and second, crystallization and growth controlled by diffusion of Cu and Zn to the interface. During the crystallization at the interface, the growth of three IMC layers (CuZn, Cu_5Zn_8, and $CuZn_4$) inside the Cu_5Zn_8 in places with fast paths for Cu diffusion starts the formation of Al_4Cu_9, which is in agreement with the Al–Cu–Zn phase diagram.[19] Further increases in time and temperature lead to growth of most of the Cu_5Zn_8 layer, as presented in Figs. 2–6. Nevertheless, other factors are also important in the nucleation and growth of phases during wetting. These include dissolving or high diffusion of Cu to the interface and solder. This reasoning is more suitable for aging of already existing solid phases,[24] where under conditions of constant temperature over time the system tends to the minimum Gibbs energy, thus promoting growth of the least energetic phase at the expense of more energetic phases. Lee et al.[25] and Wang et al.[26] showed that the phase with highest energy of formation is consumed by phases with lower energy under the specific condition that diffusion, not stability of the phases, plays the decisive role. Considering this issue for the binary Al–Zn system, where growth of the Al-rich phase at grain boundaries is controlled by volume diffusion in the matrix phase,[27] as well as other factors such as increased Li addition and Cu diffusion from the substrate, the problem becomes more complicated. However, Li addition to eutectic Zn-Al is sufficient to inhibit growth of the phase at the solder–substrate interface. At the same time, it significantly improves mechanical properties and does not affect the melting temperature of the alloy. The calculated diffusion rates for Al and Zn elements in the Cu

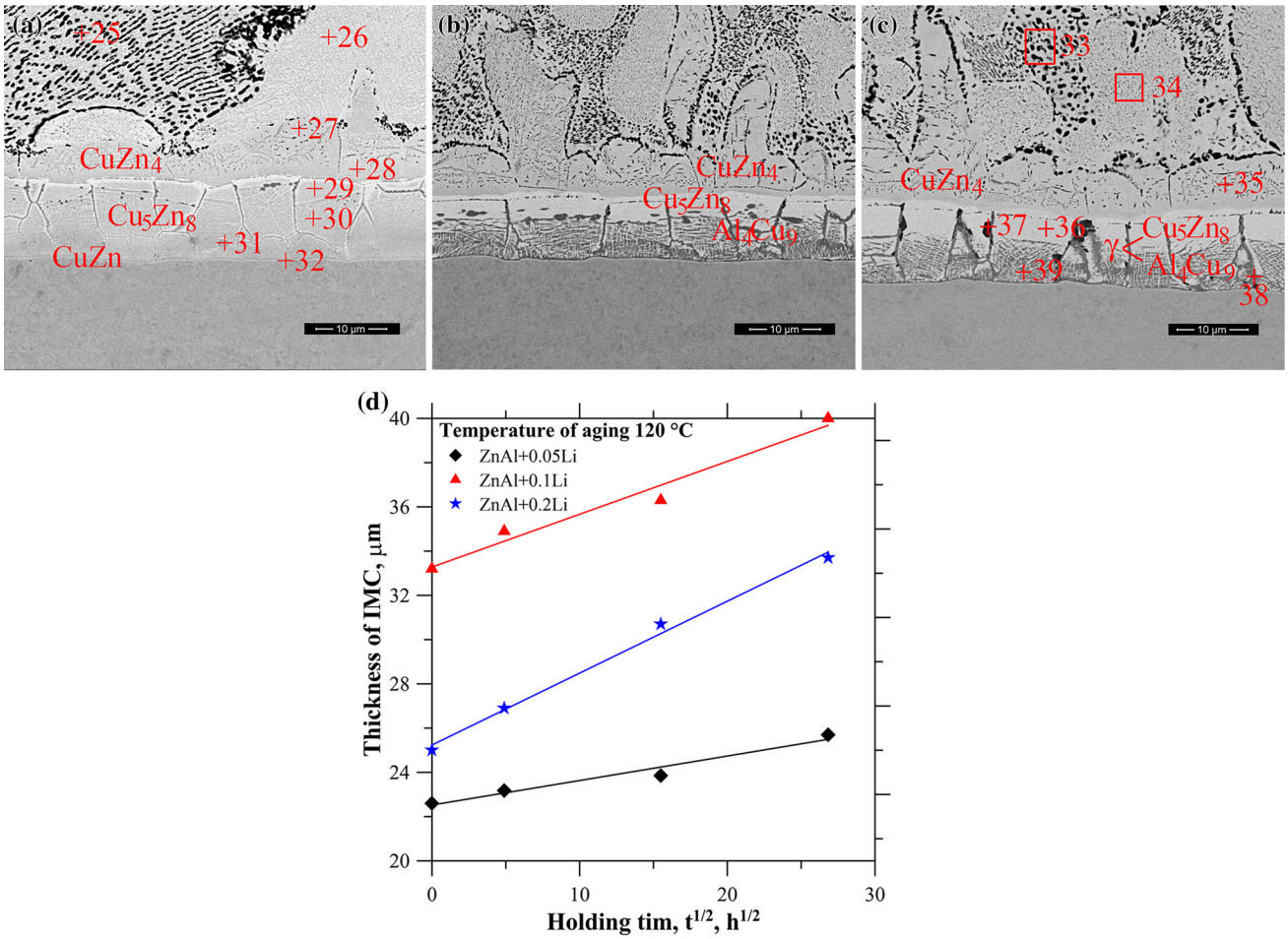

Fig. 8. Microstructure of Zn-Al + 0.05Li after aging at temperature of 250°C for (a) 1 day, (b) 10 days, and (c) 30 days, and (d) dependence of IMC layer thickness on time for Zn-Al + Li alloys after aging at temperature of 120°C, with IMCs and EDS analysis points marked (values presented in Table I).

Table III. IMC growth properties during aging in Cu/solid Zn-Al alloys with Li addition

Alloy	k (m s$^{-1/2}$)			k_0 (m s$^{-1/2}$)	Activation energy, Q (kJ mol^{-1})
	120°C	170°C	250°C		
Zn-Al + 0.05Li	1.11×10^{-10}	2.76×10^{-9}	2.24×10^{-8}	0.230	69.2
Zn-Al + 0.1Li	2.39×10^{-10}	3.11×10^{-9}	2.32×10^{-8}	0.037	61.1
Zn-Al + 0.2Li	3.25×10^{-10}	3.47×10^{-9}	3.02×10^{-8}	0.028	59.3

substrate at 450°C are 5.3×10^{14} cm^2 s^{-1} and 3.9×10^{14} cm^2 s^{-1}, respectively.[21] Furthermore, the reaction activity between the elements Al and Cu is strong,[28] in agreement with the calculations shown in Fig. 7. However, in the case of a Cu/Zn-3Al/Cu joint,[21] Al–Cu reaction products were not observed, which may be caused by the low Al content in the Zn-Al filler metal, and because the Al element is mainly dissolved in the thick Cu_5Zn_8 IMC layer.[21] This study showed that 5.3 wt.% content of Al is sufficient for formation of particles of Al_4Cu_9 in places with fast paths for Cu diffusion formed during the spreading test.

Aging Treatment

Cross sections of Zn-Al with 0.05, 0.1, and 0.2 Li content after the spreading test at 500°C for 1 min were aged for 1 day, 10 days, and 30 days at temperature of 120°C, 170°C, and 250°C. The selected samples were chosen after spreading for 1 min, to show the effect of aging time and

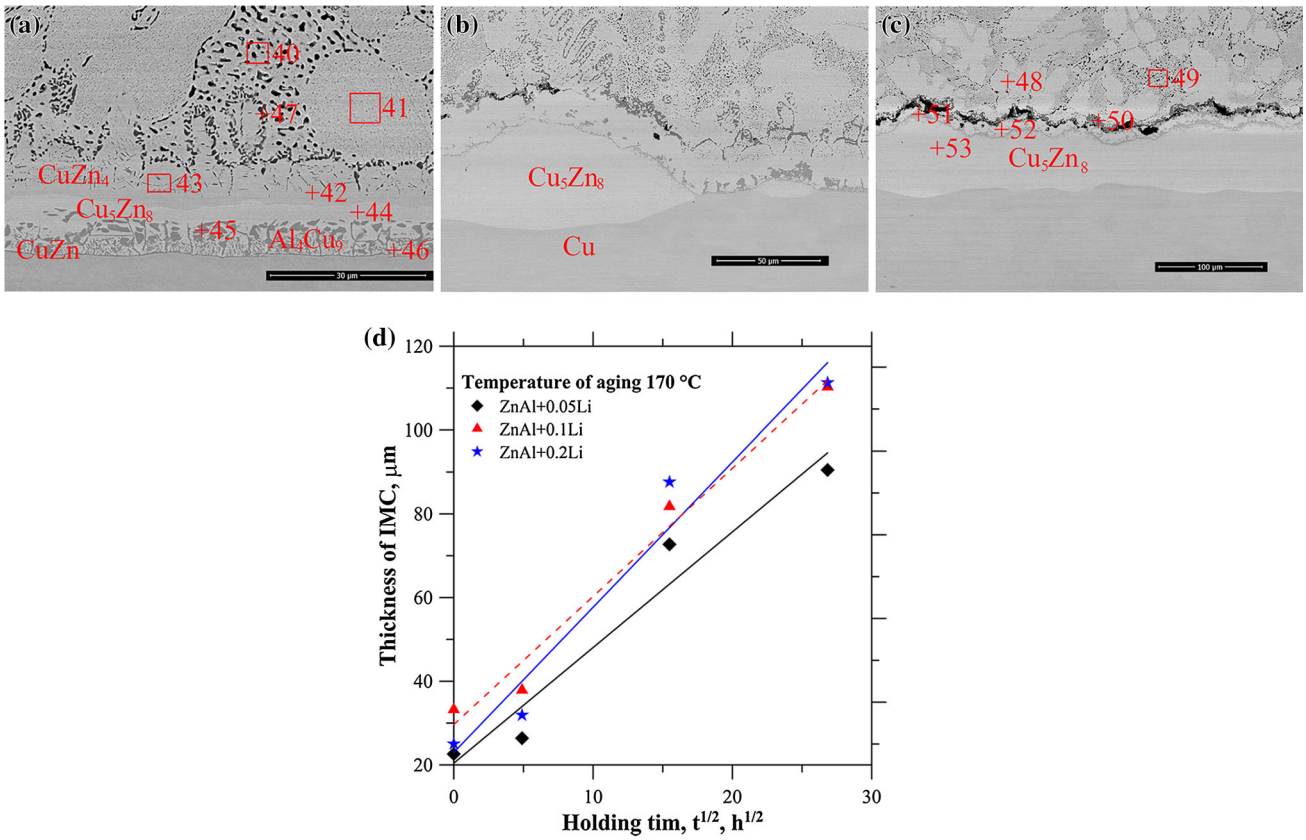

Fig. 9. Microstructure of Zn-Al + 0.05Li after aging at temperature of 250°C for (a) 1 day, (b) 10 days, and (c) 30 days, and (d) dependence of IMC layer thickness on time for Zn-Al + Li alloys after aging at temperature of 170°C, with IMCs and EDS analysis points marked (values presented in Table I).

temperature on changes occurring to the IMCs at the interface. The microstructures obtained after aging were similar for all the Zn-Al + Li alloys, with changes of the thickness of layers at the interface with differing Li content. The microstructures of Zn-Al + 0.05Li, after aging at 120°C for 1 day, 10 days, and 30 days, are presented in Fig. 8. Three layers are observed at the interface: β (CuZn), ε ($CuZn_4$), and γ (Cu_5Zn_8 and Al_4Cu_9). ε and γ grow as time increases. In the γ layer, fast Cu diffusion paths formed during the spreading test, forming Al_4Cu_9 particles that grew with increasing time and concentrated at the bottom of the layer from the Cu substrate side. According to the Al–Cu–Zn phase diagram[19] and the calculation results presented in Fig. 7, the most stable, Al_4Cu_9 phase formed at the interface. EDS analysis confirmed high concentration of Al at the interface (Table I). During aging at 120°C, the diffusion rate of Al element in the Cu substrate was slightly higher than that of Zn element,[21] which is sufficient for formation of particles of Al_4Cu_9 phase. The same situation was observed for Zn-Al + Na alloys,[12] meaning that the formed Li or Na IMCs had no effect on the creation of Al_4Cu_9 phase inside the Cu_5Zn_8 layer during aging at 120°C. However, with increased Li content in the Zn-Al + Li alloy, the IMC layers at the interface grew. The opposite effect was observed for Zn-Al + Na alloys.[12] The growth rate during aging at 120°C increased by one order of magnitude with higher Li content, as shown in Table III.

The microstructure of Zn-Al + 0.05Li, after aging at 170°C for 1 day, 10 days, and 30 days, is presented in Fig. 9. After 1 day (Fig. 9a), the microstructures of all the Zn-Al + Li alloys was similar to those after aging at 120°C, that is, two IMC layers (ε and γ), with particles of Al_4Cu_9 inside the Cu_5Zn_8 layer, as confirmed by EDS analysis (Table I). However, after 10 days (Fig. 9b), the microstructure changed. The ε-phase had been consumed by the γ-phase, and particles of the Al_4Cu_9 phase had transformed to Cu_5Zn_8. This effect is connected with the reducing concentration of Al close to the interface, which caused increasing diffusion of Cu to the solder and a greater amount of free Zn, leading to growth of the Cu_5Zn_8 layer with Al dissolving within. Independent of the stability of phases, the continuous diffusion of Cu to the interface caused changes and the growth of a less stable phase, as observed and described in Refs. 12 and 26. Wang et al.[26] found that, under specific conditions (for samples after soldering with an extremely fast cooling rate of 46°C s^{-1}), Cu_6Sn_5 and Cu_3Sn started to form during aging at 170°C for eutectic Sn-Zn with a Cu substrate (after 29 days). The Cu_5Zn_8 phase was the most stable. However,

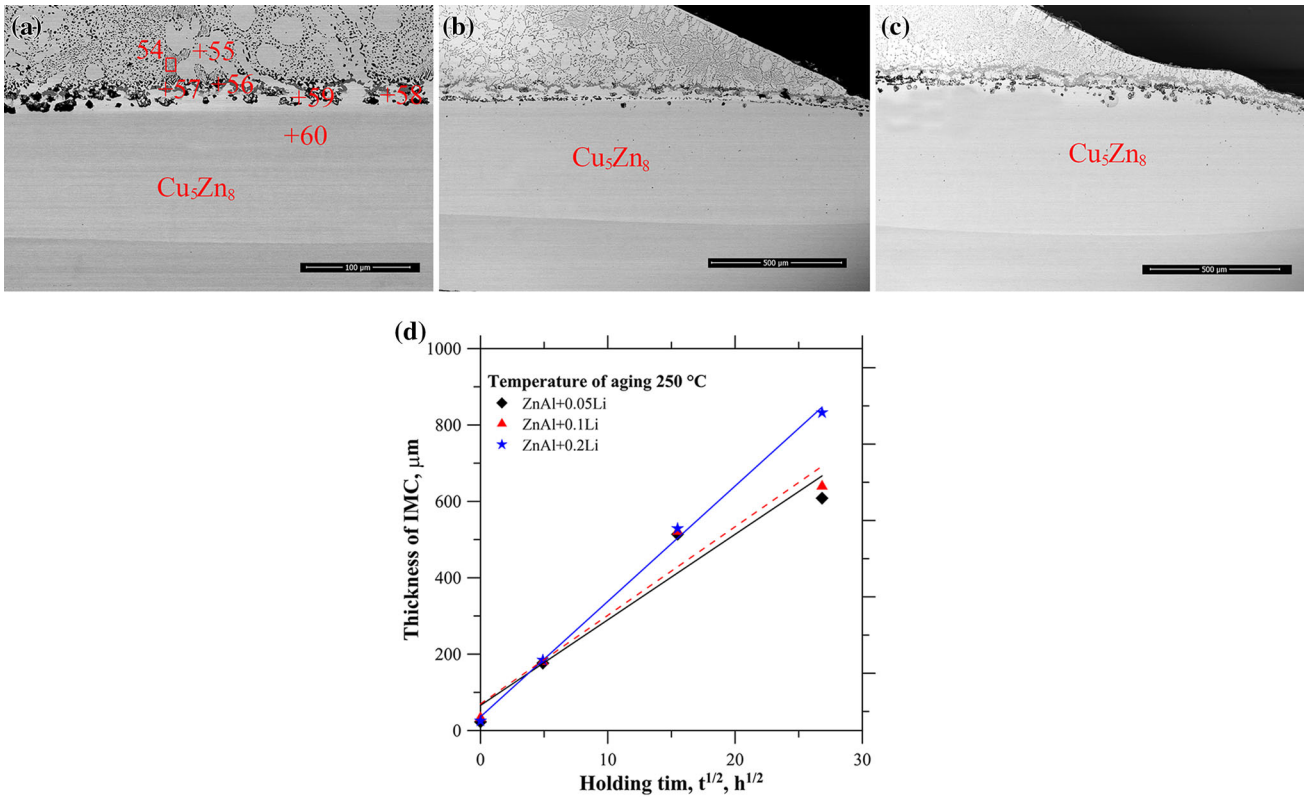

Fig. 10. Microstructure of Zn-Al + 0.05Li after aging at temperature of 250°C for (a) 1 day, (b) 10 days, and (c) 30 days, and (d) dependence of IMC layer thickness on time for Zn-Al + Li alloys after aging at temperature of 250°C, with IMCs and EDS analysis points marked (values presented in Table I).

for furnace-cooled samples, this was not observed. The same disappearance of the Al_4Cu_9 phase after 10 days was observed for Zn-Al + Na. This means that the same mechanisms take place independent of the additive. Nevertheless, addition of Li and Na has different influences on blocking the growth of IMC layers at the interface.

The microstructure of Zn-Al + 0.05Li, after aging at 250°C for 1 day, 10 days, and 30 days, is presented in Fig. 10. After 1 day (Fig. 10a), only one layer (Cu_5Zn_8) was observed, as confirmed by EDS analysis. A small particle of Al_4Cu_9 phase occurred in the top of the Cu_5Zn_8 layer. With increasing time, the Cu_5Zn_8 layer grew, and became thicker with increasing Li content (Fig. 10d). Higher growth of IMCs was observed for aging at 250°C, which correlates with the higher diffusion of Cu and Zn to the interface, causing the formation of the Cu_5Zn_8 layer. XRD analysis did not identify the occurrence of various IMC precipitates at the top of the Cu_5Zn_8 layer. Compared with Li addition, increasing Na content caused a reduction in the growth of the Cu_5Zn_8 layer, during aging at 250°C.[12] Zhu et al.[29] found that, for 90Zn-7Al-3Cu (wt.%) alloy prepared as thin films, the nanophase (Zn) decomposed during aging at 220°C for 105 h. As products of the eutectoid decomposition of the nanophase (Zn), the amount of the two phases [eutectic Zn-5.3Al and nanophase τ' 10Zn-35Al-55Cu (wt.%)] increased during further aging.[29] In this study, XRD analysis could not identify the τ'-phase. This could be because the phase is small, as the EDS analysis at point 57 revealed the possibility of the presence of fine precipitates of this τ'-phase. Comparing the effects of addition of Li versus Na[12] to eutectic Zn-Al during aging, differences were observed. Increased Li content did not block growth of IMC layers, resulting in increased thickness, whereas increasing Na addition led to a reduction in the thickness of IMC layers. Confirming the influence of Li, the activation energy (Table III) reduced with increasing Li addition to Zn-Al alloy, as opposed to increasing with additional Na (65.69 kJ mol^{-1}, 66.20 kJ mol^{-1}, and 73.11 kJ mol^{-1} for 0.2 wt.%, 0.5 wt.%, and 1.0 wt.% Na content[12]). Nevertheless, the activation energy obtained for the γ-phase during aging was much higher compared with the values of 44.37 kJ mol^{-1} for Zn-4Al[17] and 39.03 kJ mol^{-1} for Zn-4Al-1Cu.[17] For the growth rate during aging, the effect is more obvious. For aging at 120°C, the lowest value of 1.11×10^{-10} m $s^{-1/2}$ was obtained for Zn-Al-0.05Li, compared with 5.05×10^{-11} m $s^{-1/2}$ for Zn-Al-1.0Na.[12] This difference was reduced for aging at 170°C, with the lowest value of 2.76×10^{-9} m $s^{-1/2}$ being obtained for Zn-Al-0.05Li, compared with 1.72×10^{-9} m $s^{-1/2}$ for Zn-Al-1.0Na.[12] The difference was even greater for aging at 250°C, with the

lowest value of 2.24×10^{-8} m $s^{-1/2}$ being obtained for Zn-Al-0.05Li, compared with 1.40×10^{-8} m $s^{-1/2}$ for Zn-Al-1.0Na.[12] Taking into account all the parameters, Li addition to Zn-Al[12] blocks growth of IMC layers at the interface during aging, but Na addition has a much more significant effect, as observed at 250°C in the IMC layer thickness (586 μm for Zn-Al-0.05Li, compared with 399 μm for Zn-Al-1.0Na).[12]

CONCLUSIONS

Considering the conclusion of Ref. 30, further research and development for Zn-based high-temperature solders is essential for replacement of conventional Pb-based high-temperature solders. The proposed Zn-Al alloys have applications in the automotive, refrigeration, air, and space industries, and the following conclusions can be drawn:

- Li addition to eutectic Zn-Al alloy caused the spreading area to increase, with a reduction in the thickness of IMC layers at the interface during spreading tests as a function of temperature and time.
- Identification of IMCs from the Cu–Zn system, such as CuZn, Cu_5Zn_8, and $CuZn_4$ phases, formed at the interface was possible based on XRD analysis and SEM and TEM microstructure analyses of this alloy. Occurrence of IMCs from the Al–Li, Li–Zn, and Al–Li–Zn systems was also confirmed, but without literature and crystal structure data, it is impossible to identify the IMC precipitates occurring for the cast Zn-Al-Li alloys.
- For the CuZn and $CuZn_4$ phases, linear dependence of the growth of IMC over time was observed. Therefore, assuming that the exponent $n = ½$, this means that we have volume diffusion. However, for the Cu_5Zn_8 phase, it was $n \gg ½$, which corresponds to a chemical reaction in the formation process of the Cu_5Zn_8 layer. The highest activation energy was obtained for the Cu_5Zn_8 phase, being 142.6 kJ/mol for Zn-Al-0.2Li (wt.%).
- Li addition to eutectic Zn-Al did not block the growth of IMC layers during aging treatment, even resulting in faster growth with increasing Li content, which also correlated with the reduction in the activation energy of the Cu_5Zn_8 phase with increasing Li content. The highest growth was observed for aging at 250°C, where the Cu_5Zn_8 phase was dominant, which is in accordance with the Gibbs energy calculated for this phase.

ACKNOWLEDGEMENTS

This work was financed by Ministry of Science and High Education of Poland Grant IP2014 011473 “Effect of addition of Na, Li and Si to eutectic ZnAl alloys on phenomena occurring at the interface of soldered joints,” in the years 2015–2017.

OPEN ACCESS

REFERENCES

1. B.C. Wei, C.Q. Chen, Z. Huang, and Y.G. Zhang, *Mater. Sci. Eng. A* 280, 161 (2000).
2. Y. Deng, J. Yang, S. Li, J. Zhang, and X. Zhang, *Trans. Nonferr. Met. Soc.* 24, 1653 (2014).
3. R. Li, F. Pan, B. Jiang, Q. Yang, and A. Tang, *Mater. Des.* 46, 922 (2013).
4. R. Li, F. Pan, B. Jiang, H. Dong, and Q. Yang, *Mater. Sci. Eng. A* 562, 33 (2013).
5. Y. Kim, J. Kim, H. Yu, J. Choi, and H. Son, *J. Alloys Compd.* 583, 15 (2014).
6. H. Son, Y. Kim, D. Kim, J. Kim, and H. Yu, *J. Alloys Compd.* 564, 130 (2013).
7. T. Gancarz and G. Cempura, *Mater. Des.* 104, 51 (2016). doi:10.1016/j.matdes.2016.05.
8. H. Qin, H. Zhang, and H. Wu, *Mater. Sci. Eng. A* 626, 322 (2015).
9. W. Hu, Y. Liu, D. Li, X. Zeng, and C. Xu, *Phys. B* 427, 85 (2013).
10. T. Gancarz, J. Pstruś, P. Fima, and S. Mosińska, *J. Alloys Compd.* 582, 313 (2014).
11. T. Gancarz, J. Pstruś, S. Mosińska, and S. Pawlak, *Metall. Mater. Trans. A* 47, 368 (2016).
12. T. Gancarz, J. Pstruś, and K. Berent, *J. Mater. Eng. Perform.* (2016). doi:10.1007/s11665-016-2075-7.
13. C. Guo, Y. Liang, C. Li, and Z. Du, *Calphad* 35, 54 (2011).
14. S.G. Protasova, O.A. Kogtenkova, B.B. Straumal, P. Zięba, and B. Baretzky, *J. Mater. Sci.* 46, 4349 (2011).
15. G. Zeng, S. McDonald, and K. Nogita, *Microelectron. Reliab.* 52, 1306 (2012).
16. N. Kang, H. Na, S. Kim, and C. Kang, *J. Alloys Compd.* 467, 246 (2009).
17. Y. Takaku, L. Felicia, I. Ohnuma, R. Kainuma, and K. Ishida, *J. Electron. Mater.* 37, 314 (2008).
18. T. Shimizu, H. Ishikawa, I. Ohnuma, and K. Ishida, *J. Electron. Mater.* 28, 1172 (1999).
19. V. Raghavan, *J. Phase Equilib. Diff.* 28, 183 (2007).
20. T. Gancarz, *Fluid Phase Equilib.* 427, 97 (2016). doi:10.1016/j.fluid.2016.06.045.
21. Y. Xiao, M. Li, L. Wang, S. Huang, X. Du, and Z. Liu, *Mater. Des.* 73, 42 (2015).
22. K. Berent, J. Pstrus, and T. Gancarz, *J. Mater. Eng. Perform.* (2016). doi:10.1007/s11665-016-2074-8.
23. M. Date, T. Shoji, M. Fujiyoshi, K. Sato, and K.N. Tu, *Scr. Metall.* 51, 641 (2004).
24. Y.H. Zhu and J.J. Islas, *J. Mater. Process. Technol.* 66, 244 (1997).
25. H. Lee, S. Yoon, and B. Lee, *J. Electron. Mater.* 27, 1161 (1998).
26. J.Y. Wang, C.F. Lin, and C.M. Chen, *Scr. Mater.* 64, 633 (2011).
27. G. López, E. Mittemeijer, and B. Straumal, *Acta Mater.* 52, 4537 (2004).
28. J. Lee, K. Kim, K. Suganuma, J. Takenaka, and K. Hagio, *Mater. Trans.* 46, 2413 (2005).
29. Y. Zhu, W. Lee, and S. To, *Mater. Charact.* 52, 217 (2004).
30. M. Islam and A. Sharif, *Reference Module in Materials Science and Materials* (2016). doi:10.1016/B978-0-12-803581-8.04012-1.